



HAL
open science

Differential RCS of Multi-State Transponder

Arnaud Voisin, Anton Dumas, Nicolas Barbot, Smail Tedjini

► **To cite this version:**

Arnaud Voisin, Anton Dumas, Nicolas Barbot, Smail Tedjini. Differential RCS of Multi-State Transponder. 2022 Wireless Power Week (WPW), Jul 2022, Bordeaux, France. pp.195-198, 10.1109/WPW54272.2022.9853941 . hal-04009066

HAL Id: hal-04009066

<https://hal.science/hal-04009066v1>

Submitted on 28 Feb 2023

HAL is a multi-disciplinary open access archive for the deposit and dissemination of scientific research documents, whether they are published or not. The documents may come from teaching and research institutions in France or abroad, or from public or private research centers.

L'archive ouverte pluridisciplinaire **HAL**, est destinée au dépôt et à la diffusion de documents scientifiques de niveau recherche, publiés ou non, émanant des établissements d'enseignement et de recherche français ou étrangers, des laboratoires publics ou privés.

Differential RCS of Multi-State Transponder

Arnaud Voisin, Anton Dumas, Nicolas Barbot, Smail Tedjini
Univ. Grenoble Alpes, Grenoble INP, LCIS,
F-26000 Valence, France.
nicolas.barbot@lcis.grenoble-inp.fr

Abstract—This paper presents an analytical model to characterize the performance of multi-state modulation used by IQ modulators in backscatter communication. The definition of the differential RCS, originally used in the RFID technology for two states modulation, is extended to N states and allows one to characterize and compare the performance of different transponders. Read range can also be directly extracted theoretically from the internal impedance of the device. All the results are confirmed considering a transponder based on a PIC architecture. Multi-state modulation is obtained by changing the configuration of two GPIOs directly connected to a dipole antenna, in real time during runtime. Obtained delta RCS is compared to the one of classical UHF tags for passive and semi-passive technology. Associated read range is estimated in real environment.

Index Terms—Backscatter communication, differential radar cross-section (RCS), general-purpose input/output (GPIO), micro-controller (MCU), quadrature amplitude modulation (QAM), RFID.

I. INTRODUCTION

Classical transmitters rely on a local oscillator and a power amplifier to generate a continuous wave at a given frequency. Modulation is then applied to modify, the amplitude and/or phase of the carrier as a function of time to transmit the data. Since these components are active devices, transmitters also require an energy source.

However, a different architecture has been introduced able to transmit information without involving the generation of the carrier [1]. The most famous application is of course the RFID technology in which a single chip is able to harvest the energy coming from the incident wave and use it to modulate the reflected signal. This principle comes at the price of a reduced read range compared to active transmitters but allows to drastically reduce the complexity and power consumption of the transponder.

Backscatter modulation used in any UHF tag is actually done by changing the impedance value of the load connected to the antenna. Note that this change can affect both amplitude and phase of the backscattered signal. Even if classical RFID tags use only two different states, multi-state modulations have been already investigated in the literature to increase backscatter data rate and spectral efficiency. In [2], authors use 4-QAM and 8-QAM modulations. In [3] and [4], the same authors extend the results to 16-QAM modulation. Finally, N-PSK modulation is addressed in [5].

Recently, a remarkable paper [6] has opened a lot of new perspectives since the authors show that the load modulation can be done by any micro-controller simply by connecting an antenna to the GPIO of the MCU. This principle allows one to

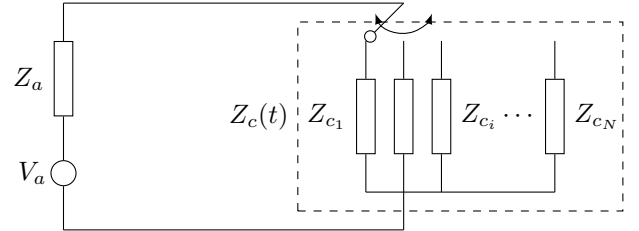


Fig. 1. Equivalent circuit of a minimum scattering antenna loaded by multi-state load. Load can be switched to N different states.

backscatter a message to a reader without using any additional component. This work has been extended to multi-state vector modulation (4-QAM) in [7].

This paper presents an analytical model to characterize the performance of multi-state transponders. This model allows to determine the delta RCS associated to the transponder and can be applied for all multi-state modulations. Read range of the system can also be directly extracted from the internal impedance values of the device. All the results are confirmed considering a multi-state transponder based on a PIC architecture. Obtained delta RCS is compared to the one of classical UHF tags for passive and semi-passive technology.

II. ANALYTICAL MODEL

The analytical model chosen to describe the performance of the signal backscattered by a multi-state transponder relies on the concept of the differential RCS. This quantity has been introduced in [8] for UHF tags which can switch their impedance between 2 different states. This section generalizes the differential RCS to N states.

Like in [8], we model the transponder antenna as a lossless minimum scattering antenna. These antennas can be described by a simple serial circuit where V_a is the voltage produced by the antenna, Z_a is the impedance of the antenna and Z_c the impedance of the transponder which depends on the considered state. Note that the backscattered power corresponds to the power dissipated in R_a (which is the real part of Z_a). If the transponder change its state, the value of Z_c is switched between the N complex impedance states Z_{c_i} with associated power wave reflection coefficient Γ_i of respective probabilities p_i and becomes a function of time. Here, we consider all signals which depend on time as stochastic processes. Thus,

the complex envelope of the current flowing into R_a can be written:

$$I(t) = \frac{V_a}{Z_a + Z_c(t)} = \frac{V_a}{2R_a} [1 - \Gamma(t)] \quad (1)$$

where $\Gamma(t)$ is the power wave reflection coefficient [9]:

$$\Gamma(t) = \frac{Z_c(t) - Z_a^*}{Z_c(t) + Z_a} \quad (2)$$

Applying the same procedure described in [10], $\Gamma(t)$ can always be decomposed into a constant part Γ_s and a variable part $\Gamma_d(t)$ with $\Gamma(t) = \Gamma_s + \Gamma_d(t)$ with:

$$\Gamma_s = \sum_i p_i \Gamma_i \quad \text{and} \quad \Gamma_d(t) = \Gamma(t) - \Gamma_s \quad (3)$$

where Γ_s corresponds to the expectation of $\Gamma(t)$ and $\Gamma_d(t)$ is a centered continuous time and discrete amplitude $\{\Gamma_i - \Gamma_s\}$ stochastic process which depends on the transmitted data and the modulation used by the transponder. We also assume that $\Gamma_d(t)$ is a wide-sense stationary and ergodic process.

The modulated power, P_{bsd} backscattered by the transponder which corresponds to the modulated power dissipated by R_a , can be expressed as:

$$P_{bsd} = \frac{V_a^2 G}{8R_a} \left[\sum_i p_i |\Gamma_i - \Gamma_s|^2 \right]. \quad (4)$$

Finally, the delta RCS associated to the multi-state transponder is equal to:

$$\sigma_d = \frac{\lambda^2 G^2}{4\pi} \left[\sum_i p_i |\Gamma_i - \Gamma_s|^2 \right]. \quad (5)$$

This delta RCS allows to characterize the modulated power generated by any multi-state backscatter modulation. Note that the second term of (5) is equal to the variance of the stochastic process $\Gamma(t)$.

The analysis of (5) allows one to see interesting properties of multi-state backscatter modulations. The delta RCS is only function of the variation of $\Gamma(t)$ with respect to its expectation Γ_s . Assuming a uniform probability distribution, the maximization of σ_d implies to have states Γ_i which are significantly different than Γ_s . For example, BPSK, 4-QAM and N-PSK (assuming equally spaced Γ_i and the same $|\Gamma_i - \Gamma_s|$ value for all states) are characterized by the same (maximum) delta RCS. Any other QAM modulations has a reduced σ_d since $|\Gamma_i - \Gamma_s|$ cannot be maximum for all points. On the other side, if a single state Γ_i has a probability of 1 delta RCS is minimum and equal to 0 since the transponder does not modulate the backscattered signal.

Moreover, assuming $|\Gamma_i| \leq 1$, (5) can be bounded by:

$$\sigma_d \leq \frac{\lambda^2 G^2}{4\pi} \left[\sum_i p_i |\Gamma_i| - |\Gamma_s|^2 \right]. \quad (6)$$

Finally, read range of the multi-state transmission is directly linked to this delta RCS and will be presented in the next section.

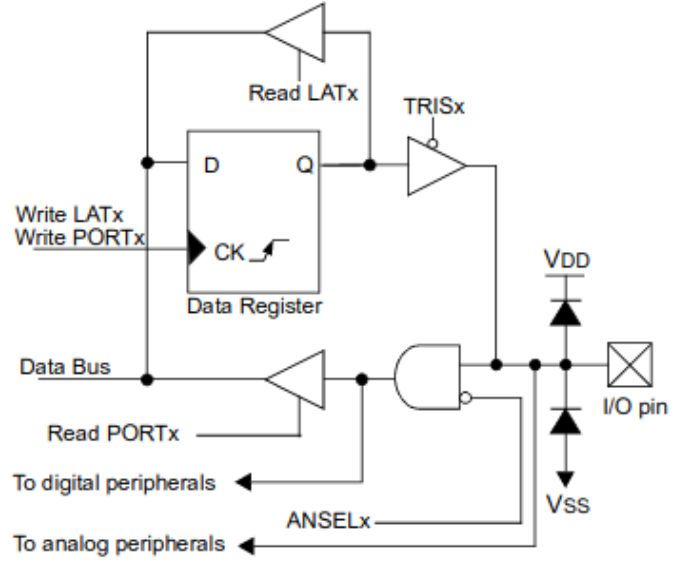


Fig. 2. Structure of the GPIO for the PIC12LF1552 MCU [11, Fig.11-1].

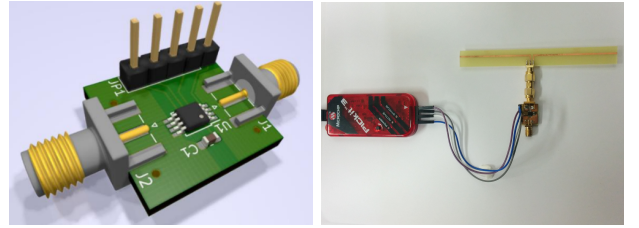


Fig. 3. (a) Printed circuit board of the multi-state transponder based on a PIC12LF1552 MCU. (b) Photograph of the transponder with the dipole antenna and the programmer/debugger kit.

III. RESULTS

A. Prototype

To validate the proposed model, a multi-state transponder has been designed based on a PIC micro-controller. The exact model is a PIC12LF1552 [11], provided in a simple 8-pin package. The structure of a GPIO is presented in Fig. 2. This GPIO structure supports 4 different modes: Analog Input (AI), Digital Input (DI) and Push Pull (PP) (low). Note that the GPIO configuration can be changed during the execution of the MCU to realize the multi-state modulation.

The proposed prototype has been realized using a small printed circuit to connect 2 GPIOs to the 2 arms of a dipole antenna through a SMA connector. The realized prototype is presented in Fig. 3. As in [6] and [7], no matching network has been used between the chip and the SMA connector. Note that the header is used to provide power supply for the MCU and to write the firmware onto the flash memory. Finally, the second SMA connector (which was connected to another GPIO) was not used during all the measurements.

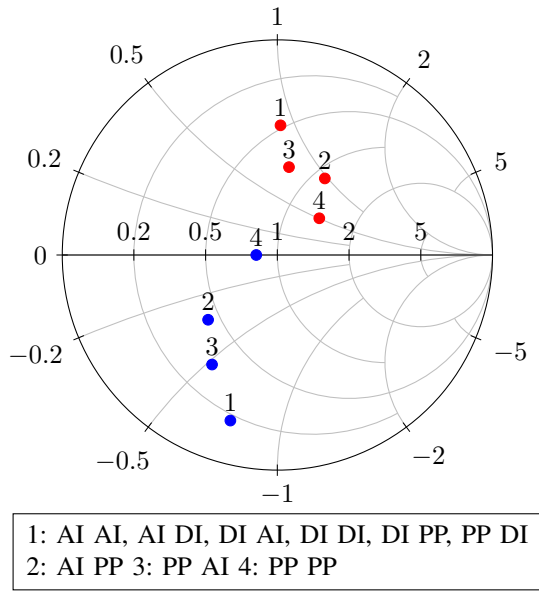


Fig. 4. Smith chart at 915 MHz (blue points) and 2.4 GHz (red points) measured at the VNA ($Z_0 = 50 \Omega$).

B. Impedance Characterization

The realized board has been characterized using a Vector Network Analyzer (VNA) to determine the impedance of the MCU for different GPIO configurations. Fig 4 presents the normalized impedance (in magnitude and phase) measured by the VNA at a frequency of 915 MHz and 2.4 GHz. Note that over the 9 possible combinations, only 4 are characterized by different impedance values. In the following, we restrict the different configurations to these 4 states (AI AI, AI PP, PP AI and PP PP). Finally, note that Γ measured by the VNA implicitly assumes that the considered antenna is perfectly matched [*i.e.* in (2), $Z_a = Z_0 = 50 \Omega$]. If the considered antenna is not matched over the entire bandwidth, (2) has to be estimated with the correct Z_a values.

C. Delta RCS

From the results presented in Fig. 4, the delta RCS, σ_d , associated to the transponder (connected to a perfectly matched minimum scattering antenna) and a uniform probability for the 4 symbols can be estimated using (5) and is respectively equal to:

$$\sigma_d = -27.0 \text{ dBsm} (20 \text{ cm}^2) \text{ at } 915 \text{ MHz} \quad (7)$$

and:

$$\sigma_d = -39.8 \text{ dBsm} (1 \text{ cm}^2) \text{ at } 2.4 \text{ GHz}. \quad (8)$$

Note that these values can easily be compared to the maximum theoretical delta RCS of RFID tags given by [10]:

$$\sigma_d = \frac{\lambda^2 G^2}{4\pi} \frac{|\Gamma_1 - \Gamma_2|^2}{4}. \quad (9)$$

Note that a factor 4 is present in the denominator to satisfy the energy conservation principle. This point is addressed in [10]. A simple numerical application shows that, at 915 MHz, (9)

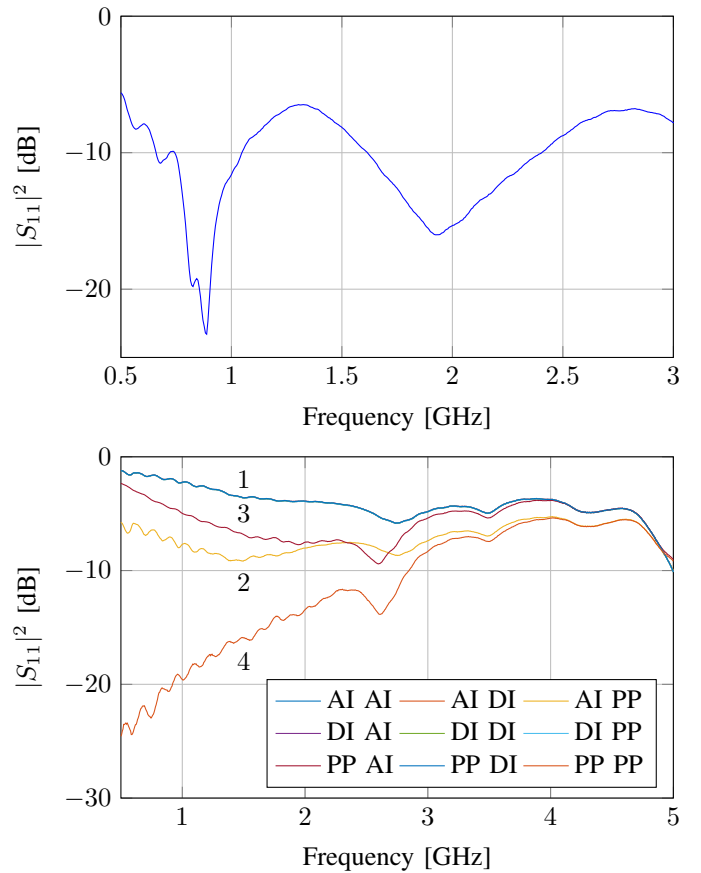


Fig. 5. Magnitude of the S_{11} measured at the VNA ($Z_0 = 50 \Omega$) for (a) the dipole antenna (b) all the GPIO configurations.

predicts a maximal delta RCS for passive (*i.e.*, $\{\Gamma_1 = 0; \Gamma_2 = -1\}$) and semi-passive (*i.e.*, $\{\Gamma_1 = +1; \Gamma_2 = -1\}$) tags of -22 dBsm (63 cm^2) and -16 dBsm (250 cm^2) respectively. Note that the values predicted by (9) correspond to the upper bound since real tags impedance states are not perfect open-circuit, short circuit or matched load. Classical values are in-between -25 dBsm (31 cm^2) and -35 dBsm (3.1 cm^2) for passive tags [8], [10]. Thus the multi-state modulation done by the proposed prototype and passive RFID tag have comparable (or slightly lower) delta RCS.

Previous discussion also considers a perfectly matched minimum scattering antenna since Γ was computed considering $Z_a = Z_0 = 50 \Omega$. The rest of this paper relaxes this assumption by considering a real half-wavelength dipole antenna realized on FR4 substrate with a SMA connector (without balun), see Fig. 3(b). Measurement of this antenna at the VNA is presented in Fig. 5(a) and shows a S_{11} parameter lower than -10 dB in the bandwidth of 750 MHz to 1 GHz. Reflection coefficient of the MCU has also been measured over a bandwidth of 500 MHz to 3 GHz and is presented in Fig. 5(b). We can see that backscatter modulation is possible for all carrier frequencies since impedance state are significantly different from each other over the full bandwidth.

Finally, Fig. 6 presents the delta RCS estimated using (5)

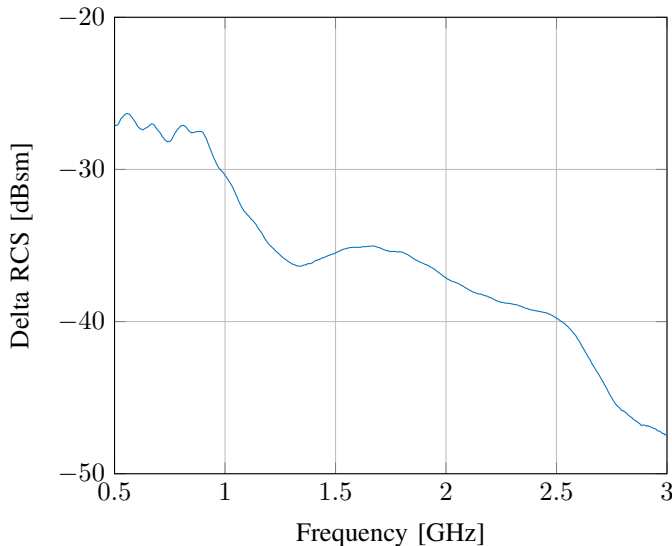


Fig. 6. Delta RCS of the multi-state modulation as a function of the frequency considering a dipole antenna.

and (2) (which considers the realistic impedance of the antenna). Note that the value at 915 MHz (*i.e.*, -28 dBsm) is close to the one obtained with the VNA [see (7)] which could not be the case for other frequencies due to the mismatch of the antenna.

D. Read Range

The evaluation of the delta RCS also allows one to directly estimate the read range of the proposed transponder. Assuming that the MCU is powered by an external source (*i.e.*, energy harvesting is not required at the transponder side), the read range in non-isolated channels is limited by the sensitivity of the reader and is given by [12]:

$$d \leq \sqrt[4]{\frac{P_t G_t G_r \lambda^2 \sigma_d}{(4\pi)^3 P_{rr \min}}} \quad (10)$$

where P_t and $P_{rr \min} = 2N_0 b$ are the transmitted power and the receiving reader sensitivity respectively (*i.e.*, the minimal differential backscattered power which can be detected).

Finally, the differential RCS introduced in this paper (and the corresponding read range) is able to characterize the performance of any multi-state transponder. Thus, comparison between different transponders can easily be realized. Table I presents the performance of the different multi-state transponders in term of delta RCS obtained from (5) and read range obtained from (10) (assuming a frequency of $f_0 = 915$ MHz, an effective isotropic radiated power of $P_t G_t = 36$ dBm and a receiving gain and sensitivity of 1 and -60 dBm respectively). One can verify that σ_d generally decreases when an higher number of state is considered. Moreover, σ_d also decreases if a given subset of the Smith chart is not used, see constellations with capacitance and inductance (LC) compared to capacitance only (C) which is in agreement with (5). Also, transponders where impedance values can be accurately selected produce

TABLE I
PERFORMANCE OF MULTI-STATE TRANSPONDERS

Reference	Modulation	σ_d (dBsm)	d (m)
[2]	4-QAM (C)	-25.4	5.0
[2]	4-QAM (LC)	-19.4	7.1
[2]	8-QAM (C)	-26.7	4.6
[2]	8-QAM (LC)	-20.6	6.6
[3]	16-QAM (C)	-21.9	6.1
[6]	BPSK (PIC)	-16.5	8.3
[6]	BPSK (AVR)	-23.9	5.4
[6]	BPSK (FPGA)	-22.2	6.0
[7]	4-QAM (EFM8)	-34.4	3.0
This work	4-QAM (PIC)	-27.0	4.6

also an higher delta RCS compared to MCU based transponders where impedance values can not be accurately controlled. Thus, delta RCS represents a important metric to characterize the performance of any multi-state transponder.

IV. CONCLUSION

This paper presents an analytical model to characterize the performance of multi-state modulation used in backscatter communications. The definition of the differential RCS, originally introduced for the RFID technology, is extended to N states. All the results are confirmed considering a multi-state transponder based on a PIC architecture. We show that this transponder is characterized by a delta RCS of -27 dBsm in the ISM band, and can be read at a distance of 4 m.

REFERENCES

- [1] H. Stockman, "Communication by means of reflected power," *Proceedings of the IRE*, vol. 36, no. 10, pp. 1196–1204, Oct. 1948.
- [2] S. Thomas and M. S. Reynolds, "QAM backscatter for passive UHF RFID tags," in *2010 IEEE International Conference on RFID (IEEE RFID 2010)*, Orlando, FL, USA, Apr. 2010, pp. 210–214.
- [3] S. J. Thomas and M. S. Reynolds, "A 96 Mbit/sec, 15.5 pJ/bit 16-QAM modulator for UHF backscatter communication," in *2012 IEEE International Conference on RFID (RFID)*, Orlando, FL, USA, Apr. 2012, pp. 185–190.
- [4] S. J. Thomas, E. Wheeler, J. Teizer, and M. S. Reynolds, "Quadrature amplitude modulated backscatter in passive and semipassive UHF RFID systems," *IEEE Trans. Microw. Theory Techn.*, vol. 60, no. 4, pp. 1175–1182, 2012.
- [5] J. Qian, A. N. Parks, J. R. Smith, F. Gao, and S. Jin, "IoT communications with M-PSK modulated ambient backscatter: Algorithm, analysis, and implementation," *IEEE Internet of Things Journal*, vol. 6, no. 1, pp. 844–855, Feb. 2019.
- [6] A. Dadkhah, J. Rosenthal, and M. S. Reynolds, "Zeroscatter: Zero-added-component backscatter communication using existing digital I/O pins," in *2019 IEEE Topical Conference on Wireless Sensors and Sensor Networks (WiSNet)*, Orlando, FL, USA, Jan. 2019, pp. 1–3.
- [7] S. J. Thomas and J. A. Howe, "Achieving multistate vector scattering with unmodified digital input/output pins," *IEEE Journal of Radio Frequency Identification*, vol. 5, no. 3, pp. 311–316, Sep. 2021.
- [8] P. V. Nikitin, K. V. S. Rao, and R. D. Martinez, "Differential RCS of RFID tag," *Electron. Lett.*, vol. 43, no. 8, pp. 431–432, Apr. 2007.
- [9] K. Kurokawa, "Power waves and the scattering matrix," *IEEE Trans. Microw. Theory Techn.*, vol. 13, no. 2, pp. 194–202, Mar. 1965.
- [10] N. Barbot, O. Rance, and E. Perret, "Differential RCS of modulated tag," *IEEE Trans. Antennas Propag.*, vol. 69, no. 9, pp. 6128–6133, Sep. 2021.
- [11] Microchip PIC12LF1552. [Online]. Available: ww1.microchip.com/downloads/en/DeviceDoc/40001674F.pdf
- [12] N. Barbot, O. Rance, and E. Perret, "Classical RFID versus chipless RFID read range: Is linearity a friend or a foe?" *IEEE Trans. Microw. Theory Techn.*, vol. 69, no. 9, pp. 4199–4208, Sep. 2021.